ELSEVIER

Spectrochimica Acta Part B 52 (1997) 2151–2161

SPECTROCHIMICA
ACTA
PART B

Simultaneous multielemental determination using a low-resolution inductively coupled plasma spectrometer/diode array detection system

Maria Fernanda Pimentel[a],*, Benício de Barros Neto[b], Mário César Ugulino de Araújo[c], Célio Pasquini[d]

[a]*Fundação Instituto Tecnológico do Estado de Pernambuco-ITEP, Av. Prof. Luís Freire, 700-Cidade Universitária, 50740-540 Recife, PE Brasil*
[b]*Departamento de Química Fundamental, CCEN, Universidade Federal de Pernambuco, 50739-907, Recife, PE, Brasil*
[c]*Departamento de Química, CCEN, Universidade Federal da Paraíba, João Pessoa, PB, Brasil*
[d]*Instituto de Química, Universidade Estadual de Campinas, UNICAMP, Campinas, SP, Brasil*

Abstract

This work presents a versatile method for simultaneous multielemental analysis using detection with photodiode arrays and multivariate calibration techniques. A multidetection system based on an array of 1 024 photodiodes was built and adapted to a commercial plasma emission scanning spectrometer. Spectral data were acquired at low resolution, allowing simultaneous monitoring of a broad spectral range and resulting in very informative but considerably overlapped spectra. Partial least squares and principal component regressions were employed to minimize overlapping problems. A numerical procedure for window selection was also developed.

The new method was applied to the simultaneous determination of manganese, molybdenum, nickel, chromium and iron in steel samples, resulting in average relative prediction errors of 2.1% for Mn, 3.4% for Mo, 0.6% for Cr, 1.5% for Ni and 0.8% for Fe. These errors are comparable to those observed with conventional scanning detection systems and separate univariate calibrations, but the new method allows simultaneous determination of the five elements, with data acquisition significantly faster than in scanning instruments. © 1997 Elsevier Science B.V.

Keywords: Multivariate calibration; Plasma emission spectrometry; Photodiode array

1. Introduction

Inductively coupled plasma atomic emission spectrometry (ICP-AES) is well-established as a powerful technique for multielemental analysis [1]. The high temperature of the source minimizes matrix effects and produces adequate sensitivity for most metals and some non-metals, in concentrations ranging from percent to ppb. Also, since many intense emission lines occur for almost all elements present in a given sample, ICP-AES is essentially a simultaneous multicomponent analytical technique. Many conventional detection systems, however, are not optimized for full exploitation of the enormous amount of information produced by an ICP source.

Most of the early commercially available instruments employ detection systems based on photomultiplier tubes (PMT) [2]. The usual designs either couple one PMT with a scanning monochromator or employ a polychromator with several fixed exit slits and photomultipliers, resulting in the so-called direct-reading spectrometers [3]. Scanning

---

* Corresponding author, E-mail: fernanda@pop-pe.rnp.br

0584-8547/97/$17.00 © 1997 Elsevier Science B.V. All rights reserved
PII S0584-8547(97)00091-8

systems allow excellent flexibility in the choice of optimal analytical lines, but acquire information sequentially in narrow bandwidths. Direct-reading spectrometers, while able to monitor wide spectral ranges, and thus allow simultaneous multicomponent analysis, suffer from geometric and mechanical constraints imposed by the dimensions of a PMT that limit the minimum distance between two analytical lines monitored by the same polychromator. Further, there is no flexibility in line selection, the instrument is not easily reprogrammable to record a new set of analytical lines, and costs increase steeply with the number of monitored lines. Such instruments are best suited to high-volume runs under routine protocols for known elements.

An ideal detector for atomic emission spectrometry would combine the convenience of an eletronic readout, typical of PMTs, with the multichannel detection capability of the old photographic plates [3]. Perhaps the detection systems that come closer to having these ideal characteristics are the ones based on charge-coupled (CCD) or on charge-injection devices (CID) technologies. Coupled to a well-designed echelle optics, CCD or CID detectors exhibit the broad range/high resolution found in instruments like the Optima-3000 (Perkin-Elmer) or the Iris (Thermo Jarrell Ash) [2,4,5]. This top-of-line combination of a modern detection system with sophisticated optics proved very successful in multielemental determinations, with only a few interferences reported in the literature[6]. However, adoption of this approach is still quite expensive, leaving room for consideration of other ways of achieving multielemental determination in ICP-AES.

Image sensors such as photodiode arrays (which are inexpensive solid state multichannel detectors) were investigated extensively for use in atomic emission spectrometry with conventional spectrometers [3,7–13]. However, because of the finite width of a photodiode array these detectors require a compromise between spectral resolution and wavelength range. To increase the spectral range monitored simultaneously the dispersion has to be reduced, and this in turn leads to more spectral interferences.

The need for high-resolution systems is typical of traditional univariate calibrations, where most of the spectral information is ignored and just one or two lines are observed for each element, chosen for their relatively high intensities and freedom from spectral interferences. With the increasing availability of microcomputers capable of handling and storing large data sets, several applications of multivariate methods, which can use all the spectral information and minimize overlap problems, have started to appear in the ICP-AES literature [14–28]. Kalman filters [14–17], least squares regression [18], numerical derivatives[19,20], stepwise multiple linear regression [21], GSAM [6,22–24], matrix projections [25,6], [22–24] and factor analysis [27,28] are among the multivariate methods employed to correct for spectral interferences in ICP-AES.

Factor analysis was employed by Wirsz and Blades for qualitative and quantitative multielement analysis using a low resolution ICP spectrometer with a photodiode array detection system, in which a window of 50 nm was monitored simultaneously [28]. Factor analysis was used to identify sample components and to minimize problems arising from spectral overlap. The predicted concentrations, obtained with a nonoptimized spectral window and very low resolution, had relative errors in the range 3%–20.8%, which seem rather large considering that all the elements were present with a single, high (250 mg/L) concentration. Even so, the work of Wirsz and Blades has the considerable merit of proposing multivariate methods as a tool to strike a compromise between monitored range and spectral resolution.

In the present work a versatile method for simultaneous multielemental analysis is described, based on the use of multivariate calibration techniques to deal with spectral interferences caused by a low resolution dispersion system. Instead of factor analysis we resort to calibration in latent variables, specifically partial least squares regression (PLS) and principal component regression (PCR) [29–31], which were employed successfully to treat interferences in spectrochemical analysis [32–35]. It is suggested, as an integral step of the general procedure, a new criterion for selecting the optimal spectral window for a given application. To assess its efficiency, advantages and disadvantages, the proposed method is applied to the simultaneous determination of manganese, molybdenum, nickel, chromium and iron in steel samples.

2. Experimental

2.1. Instrumentation

A sequential ICP Spectroflame spectrometer manufactured by Spectro, converted into a multichannel system through the introduction of a multidetection system based on an array containing 1024 photodiodes, was employed [36]. In the modified system the radiation from the source is led through an optical fiber to the entrance slit of a low resolution dispersion device, in whose focal plane the multidetection system is placed. The dispersion is provided by a 1200 lines/mm diffraction grating, which allows simultaneous monitoring of a 81 nm wide window. Operating conditions are shown in Table 1.

2.2. Samples, reagents and reference solutions

1.000 mg/L stock solutions were prepared for each element by diluting Tritisol (Merck) ampoules with purified water. As recommended by the manufacturer, the iron and chromium solutions were kept in HCl 15% (v/v) and 4.2% (v/v), respectively. No acid was added to the manganese, nickel or molybdenum stock solutions.

The standard solutions used for window selection were prepared by diluting the stock solutions. The calibration mixtures and synthetic samples were also made by dilution of the stock solutions, with HCl added to maintain an acid concentration of 5% (v/v).

The steel samples were dissolved according to the following procedure. Approximately 0.5 g of homogeneized sample material was weighed, treated with 9 mL of HCl (1:1) and put in a water bath for 1 hour. 3 mL of HNO_3 (1:1) were then added, and the sample was returned to the bath for another half hour. After cooling to room temperature, the sample was filtered through quantitative filter paper. The filtrate was transferred to a 200 mL volumetric flask and the volume was completed with water. Immediately before spectral acquisition the sample was diluted 1:10 and enough HCl was added to reach an acid concentration of 5% (v/v). A blank was prepared following the same steps.

Table 1
Operating conditions of the inductively coupled plasma atomic emission spectrometer.

Argon flow	12 L min^{-1} (coolant) 0.5 L min^{-1} (auxiliary) 1.0 L min^{-1} (nebulizer)
Sample uptake rate	2.3 mL min^{-1}
RF power	1 kW
Observation height	15 mm above the coil
Integration time	1 s

To select the dissolution procedure the expected concentration ranges of the elements in typical steel samples were taken into account. Because of the limited dynamic range of the PDA, a diluting factor was chosen to strike a compromise between the detection limits for the less abundant elements and the signal saturation caused by the more concentrated elements, within 1 s integration time.

Analytical grade or suprapur (Merck) acids and water purified by a Milli-Q (Millipore) system were used throughout.

2.3. Experimental design

The concentrations of the calibration mixtures were selected according to a two-level five component mixture design including a central point, using the XVERT algorithm [37]. Seventeen different solutions were prepared as specified by the algorithm, with some minor concentration adjustments made to simplify the experimental procedures.

Table 2 shows the concentrations of the elements in each calibration mixture, in mg/L. The calibration ranges corresponding to the mixtures of Table 2 for each element in the hypothetical original steel samples would be the following:

$$\text{Mn}: 0.4-2.0\%; \quad \text{Mo}: 0.6-4.0\%; \quad \text{Cr}: 8-28\%;$$
$$\text{Ni}: 4-28\%; \quad \text{Fe}: 40-88\%$$

For model assessment we used a test set consisting of another 10 synthetic mixtures (simulating typical steel samples) plus 9 actual reference steel samples. Each reference sample was analysed three times. The chemical compositions of the nineteen test samples are presented in Table 3.

2.4. Software

Version 5.0 of the UNSCRAMBLER chemometrics software (CAMO A/S) was used for the PLS and PCR

Table 2
Compositions of the seventeen calibration mixtures specified by the XVERT algorithm for the two-level five component design.

	Concentration, mg/l				
Mixture number	Mn	Mo	Cr	Ni	Fe
1	1.0	1.5	20.0	10.0	220.0
2	5.0	1.5	20.0	10.0	220.0
3	1.0	10.0	20.0	10.0	210.0
4	5.0	10.0	20.0	10.0	210.0
5	1.0	1.5	70.0	10.0	170.0
6	5.0	1.5	70.0	10.0	170.0
7	1.0	10.0	70.0	10.0	160.0
8	5.0	10.0	70.0	10.0	160.0
9	1.0	1.5	20.0	70.0	160.0
10	5.0	1.5	20.0	70.0	150.0
11	1.0	10.0	20.0	70.0	150.0
12	5.0	10.0	20.0	70.0	150.0
13	1.0	1.5	70.0	70.0	100.0
14	5.0	1.5	70.0	70.0	100.0
15	1.0	10.0	70.0	70.0	100.0
16	5.0	10.0	70.0	70.0	100.0
17	3.0	6.0	50.0	40.0	150.0

Table 3
Percent compositions of the nineteen test samples. Lines 11–19 correspond to certified steel samples.

Sample		Composition				
No.	Origin	Mn	Mo	Cr	Ni	Fe
1	Synthetic	0.80	1.20	12.0	6.0	80.0
2	Synthetic	1.60	3.20	16.0	12.0	68.0
3	Synthetic	2.00	2.00	24.0	8.0	64.0
4	Synthetic	1.00	1.44	14.0	20.0	64.0
5	Synthetic	1.40	1.60	18.0	18.0	60.0
6	Synthetic	1.80	2.00	19.2	24.0	52.0
7	Synthetic	0.60	3.60	26.0	14.0	56.0
8	Synthetic	1.48	2.80	9.2	19.2	68.0
9	Synthetic	0.88	1.12	10.0	10.0	80.0
10	Synthetic	1.28	4.00	14.8	15.2	64.0
11	BCS 473	0.494	0.95	9.06	-	88.7
12	BCS 471	0.417	-	23.85	0.96*	73.8
13	BCS 332	0.80	-	12.8	12.4	72.6
14	BCS 341	0.43	-	24.0	0.56*	73.6
15	BCS 342	0.91	0.69	16.1	2.16*	79.4
16	BCS 464	0.77	-	25.7	20.7	52.1
17	CRM 466	0.698	2.19	17.65	8.61	70.2
18	BCS 469	0.598	-	11.93	0.246*	87.0
19	IPT-24	1.50	2.54	17.81	9.93	67.6

* Values below the lower limit of the calibration range

calculations [38]. For the window selection procedure discussed later we used programs developed in our own laboratory with the MATLAB high-level programming language [39].

3. Results and discussion

3.1. Selection of the spectral window

Most of the emission lines for the five elements analysed in this work fall between 200 and 400 nm [1] but the diode array employed for detection is able to acquire spectral data in a continuous bandwidth of only 81 nm, because a 1200 lines/mm diffraction grating is being used. The problem therefore arises of defining which 81 nm window between 200 and 400 nm is the best for the simultaneous determination of Mn, Mo, Cr, Ni and Fe. Window selection based on ICP-AES wavelength tables does not lead to good results, because the low resolution operating conditions cause a large amount of overlap that must be taken into account.

Good sense dictates that the best spectral window would be the one with the largest amount of information, which in this case means the presence of lines with intensity above the detection limit (unsaturated, of course) and also with minimum overlap. In what follows we propose a numerical criterion based on these two requisites.

The procedure is initiated by an examination of the individual spectra of the five elements. These spectra were recorded at concentrations that would approximately result from typical steel samples analyzed in a routine laboratory procedure:

200 mg/l Fe; 40 mg/l Cr; 20 mg/l Ni;

2 mg/l Mn∧5 mg/l Mo.

To cover the entire 200–400 nm spectral range with the 81 nm diode array, three spectra were acquired in three partially overlapping consecutive windows. Since at the resolution employed here the ratio between wavelength and photodiode is 0.0791 nm/diode, the full 200 nm wide spectrum contains 2 528 intensity values for each element. Each spectrum is background corrected before being subjected to further treatment.

The selection procedure starts by defining the interferent spectrum for each element as the superposition of the other four individual spectra. For example, the molybdenum interferent spectrum is the sum of the other four (Fe, Cr, Ni and Mn) pure spectra. The spectrum of a specific element together with its interferent spectrum are then used to evaluate which diodes (channels) have important information for the analytical determination of that particular element. A given channel is considered informative for the element under investigation if the recorded intensity in the pure element spectrum satisfies the following criteria.

- It is above the detection limit (three times the blank standard deviation).
- It is not saturated.
- It is at least 20% higher than the corresponding intensity in the interferent spectrum.

For each informative channel—in the sense just defined—the interferent spectral intensity is subtracted from the intensity in the element's pure spectrum and the result is divided by the intensity range over the whole pure spectrum. This results in a dimensionless parameter that can be regarded as a measure of how much the spectrum of the element in question is free from interference in that channel. This procedure is summarized by the equation

$$\Delta(i,j) = \frac{I(i,j) - \sum_{k\neq i} I(k,j)}{I_{\max}(i)} \tag{1}$$

where i and j denote the chemical element and the channel of interest, respectively. The sum is performed over the four interfering elements, denoted by k. I stands for the emission intensities. $I_{\max}(i)$ is the spectral intensity range, that is, the difference between the strongest and the weakest intensities recorded in the spectrum of element i.

If a given channel fails to meet the requisites to be considered informative for the element in question, its $\Delta(i,j)$ value is set equal to zero. This assures that each channel either will be informative for a single element, or will not be informative at all.

The 20% excess value in Eq. (1) is somewhat arbitrary. Larger values were tried but failed to yield informative regions for molybdenum. Also, Eq. (1) does not distinguish overlapped bands from those free from interference, but at this low resolution—and for the samples considered here—no region without overlapping was observed. If the need arises, different percentages can be easily implemented in the algorithm.

To see how the information in a spectral window varies with the window's location within the 200-400 nm range, the $\Delta(i,j)$ values are computed for the 2 528 channels in the range, and then summed over the 1024 diodes of each possible window. The resulting parameter measures the amount of useful information contained in the window as a whole, for the element of interest. Plots of this parameter against the initial wavelength of the corresponding window are shown in Fig. 1, for each of the five elements under investigation.

Fig. 1 shows that for manganese and molybdenum there are many spectral windows containing no useful information. The $\Delta(i,j)$ values are zero for all windows starting above 257 nm for manganese and below 236 nm for molybdenum. Only the 236-257 nm interval is informative for both elements. It turns out, however, that it is also the least informative spectral region for nickel.

To combine the information displayed in the five plots in Fig. 1 in a single parameter, we first divide the useful information in each window by the number of informative channels, obtaining the average information per channel. Then we take the geometrical mean of these averages over the five elements. The resulting parameter, denoted by $\mu(s)$, where s is the window's starting wavelength, is plotted in Fig. 2. It provides a convenient measure of how useful a given window is for the simultaneous determination of the five elements, increasing as the combined information increases, and becoming equal to zero if at least one window contains no spectral information for one of the five elements.

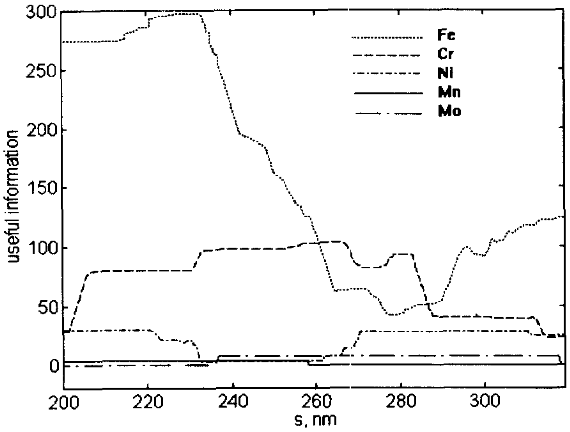

Fig. 1. Useful information from the 81 nm windows plotted against the window initial wavelengths for the five elements (Fe, Cr, Ni, Mn, Mo). s stands for the window's starting wavelength.

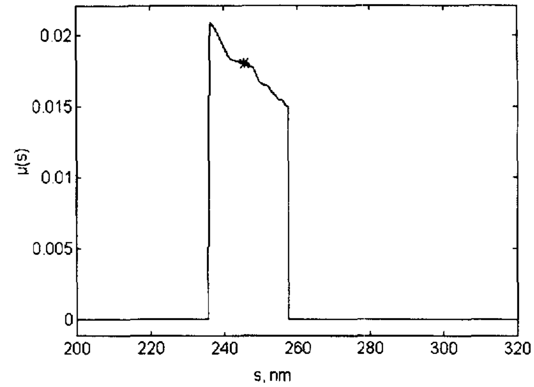

Fig. 2. Numerical measure of the usefulness of a 81 nm spectral window, $\mu(s)$, plotted against the window's starting wavelength, s. The asterisk at 245 nm indicates the working window. The algorithm for obtaining m(s) is described in the text.

The maximum of the plot in Fig. 2, corresponding to the initial wavelength of the most informative window for the five elements, occurs at 236.6 nm. If this window is chosen, however, the most informative wavelengths for molybdenum will be located at the very end of the range, that is, only the last few—and, according to the manufacturer, less reliable—photodiodes of the 1024 array would be able to record information for this element. To avoid the problem of relying on these unfavorably located diodes for Mo, we decided to work instead with the window beginning at 245 nm (and covering the spectral range up to 326 nm), a displacement made at the cost of a small loss of information for iron, as can be observed in Fig. 1. The final working window is indicated by an asterisk in Fig. 2.

This window is of course optimized for the present application. Other kinds of sample will require the optimization procedure to be done again. For samples with more elements to be analyzed the general methodology remains valid, but the experimental work may be considerably increased, and could perhaps be alleviated by the use of flow systems.

A 600 lines/mm grating was also tried. The results obtained for iron, manganese, nickel and chromium were comparable to those reported here, but the predictions for molybdenum were much worse. In any case, exchange of the gratings is very easy, if a 600 lines/mm (or, conversely, 2400 lines/mm) grating should prove to be more adequate for another application.

3.2. Data preprocessing

The spectra of the blank, calibration and test samples were recorded in the 245–326 nm working window using a integration time of one second. Each spectrum is actually the average of 5 replicates, recorded sequentially. Because of their poor reliability (large response variation, as stated by the manufacturer and also verified in practice), the intensities recorded by the first and the last four photodiodes were discarded, reducing the number of intensity values to 1 016. After exclusion of all saturated photodiodes, this number was further reduced to 723. Only then was the blank spectrum subtracted from the spectra of the other samples.

After this preprocessing step, the **X** matrix for the calibration set contained 17 objects (the seventeen calibration samples) and 723 variables (remaining wavelengths/channels). The **X** matrix for the test set was formed by 37 objects: 10 synthetic samples plus 9 reference samples analyzed in triplicate.

3.2.1. Calibration

Two calibration models were constructed, employing partial least squares regression (PLS) and principal component regression (PCR). In what follows we discuss the PLS calibration procedure in detail. For the PCR calibration, which employs a similar algorithm, we just present the results for comparison.

In both PLS and PCR the **X** matrix data were autoscaled to unit variance before calibration, as is the norm with calibrations on latent variables [29–31]. The **Y** matrix contains the concentrations of the five elements in the calibration samples. Since they are not correlated, the PLS1 method was employed and each element was modelled separately.

Several variables and three samples were classified as outliers in the **X** matrix by the UNSCRAMBLER standard procedure, based on a comparison of the relative errors of prediction with a limit specified by the user. The three outlying samples belonged to the test set and were replicates of reference samples 12, 16 and 17 in Table 3. Since the other replicates of the same samples were considered normal, we assumed that in the case of the three outliers gross errors had occurred during sample preparation and discarded them from the test set, keeping only the other two replicates. The test set was thus reduced to 34 objects.

Most of the outlying variables were located in spectral regions almost devoid of significant lines and probably represent mostly noise, somewhat amplified by the scaling procedure. These variables were submitted to a stepwise exclusion procedure in which the root mean square error of prediction (RMSEP) was continually monitored to prevent exclusion of informative diodes. In this fashion 101 more variables were discarded, and only 622 remained in the final calibration.

External and internal validation procedures were used to determine the optimal number of factors for calibration. External validation was based on RMSEP values obtained from a comparison of the predicted and the true concentrations of the test objects. For the internal procedure the program's full crossvalidation algorithm was employed. Both methods are illustrated in Fig. 3, with the results for manganese and molybdenum as examples.

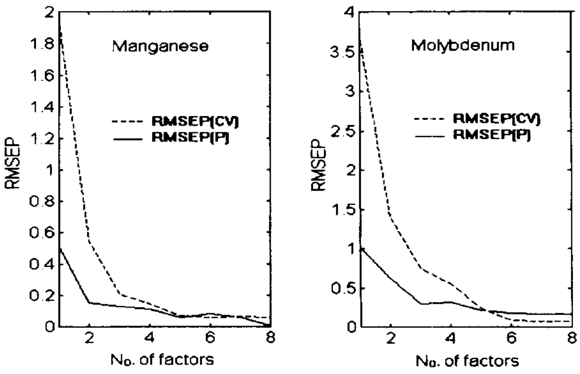

Fig. 3. RMSEP values plotted against the number of factors for the manganese and molybdenum PLS calibration models. - - - Cross-validation RMSEP [RMSEP(CV)]. —— External validation RMSEP [RMSEP(P)].

For manganese the optimal number of PLS factors is five, since after this the external validation RMSEP value starts to rise, while the crossvalidation RMSEP value remains stable. For molybdenum six factors were chosen, because adding more factors leaves both RMSEP values practically unaffected. Using the same procedure, five factors were selected for chromium, six for nickel, and three for iron.

For manganese and chromium the optimal number of factors is five in both kinds of multivariate calibration. For the other three elements the PLS calibrations require one factor less than the principal component regressions. The optimal PLS models use six factors for molybdenum and nickel and three factors for iron, in contrast with 7, 7 and 4 factors, respectively, used by the optimal PCR models. Partial least squares modelling succeeds in sometimes producing calibration models with less dimensions because the PLS algorithm concentrates on modelling **X** matrix phenomena that are correlated to those in the **Y** matrix, while the PCR algorithm ignores **Y** values when modelling **X** matrix information[29].

It is interesting that the optimal number of principal components in the regressions is not always five, as would be expected from a principal component analysis done on the intensities matrix alone. The reason seems to be that in PLS (or PCR) regression information from the concentration matrix is also introduced in the calculations. The criterion used here to choose the number of components is to look for the minimum error of prediction and of course this depends on both matrices. It is also important, for validation, that the residuals be distributed normally. No abnormal behavior was observed in the residual plots of any of the five calibration models.

3.3. Model assessment

The concentration values predicted for the test samples in the PLS calibration are compared with the true values in Fig. 4. The straight lines are the first quadrant bisectors. The agreement is excellent for all five elements, as the closeness of the points to the bisecting lines shows.

The average absolute errors of prediction of the two multivariate calibrations for the test samples are presented in Table 4. The errors obtained with five individual univariate calibrations and the equipment's original detection/dispersion system, which allows selection of individual non-overlapped lines for each element, are also included for comparison. The lines chosen for univariate calibration are the following: Ni: 231.604 nm; Mn: 257.61 nm; Cr: 267.716 nm; Mo: 281.615 nm; Fe: 297.324 nm.

The performance of the two multivariate methods is almost the same. The PLS and PCR errors are identical for iron and nearly so for manganese and molybdenum. Only for chromium and nickel are the PLS results slightly superior. The two multivariate results are also very similar to the results from the univariate calibrations. The sole exception is molybdenum, for which the PLS/PCR average error is almost twice the corresponding univariate error. This is also the case where the relative average errors are highest: 3.4%, in contrast to 2.1% for manganese, 0.6% for chromium, 1.5% for nickel and 0.8% for iron. The main reason is the heavy overlapping of the molybdenum spectrum by the spectra of the other four elements. This is illustrated in Fig. 5, where the spectrum of sample 13, which does not contain molybdenum, is compared with two pure Mo spectra corresponding to the concentration range

Table 4
Average absolute errors in the predicted concentrations of the test samples using the simultaneous multidetection system with PLS and PCR calibration, and the conventional system with univariate calibration. Errors are expressed in % concentration values.

Element	Average absolute error of prediction		
	PLS	PCR	Univariate calibration
Mn	0.018	0.016	0.017
Mo	0.051	0.053	0.028
Cr	0.097	0.118	0.107
Ni	0.173	0.196	0.221
Fe	0.505	0.505	0.656

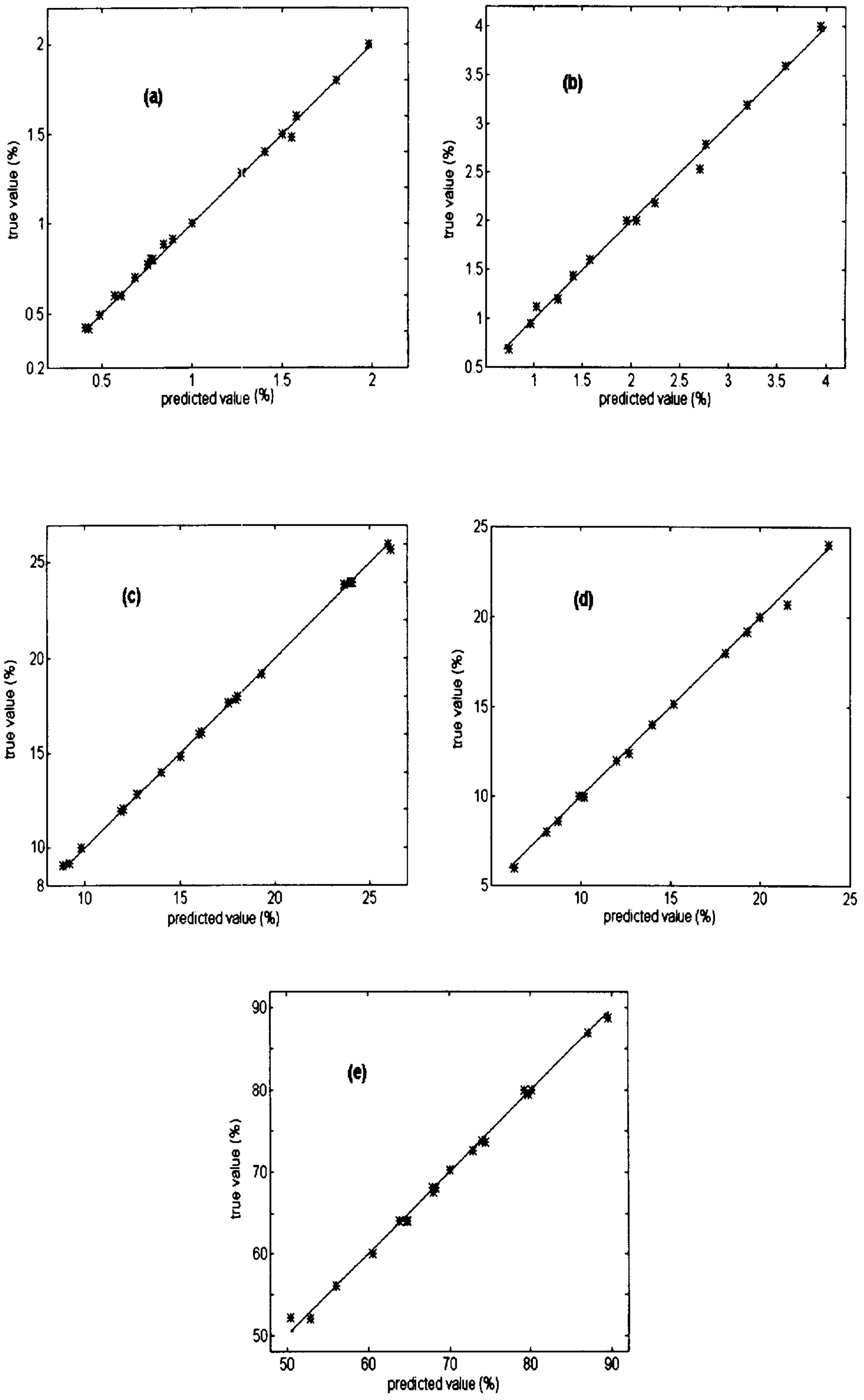

Fig. 4. Test set predicted concentration values compared with true values for the five elements. The straigth line is the first quadrant bisector. (a) Manganese; (b) Molybdenum; (c) Chromium; (d) Nickel; (e) Iron.

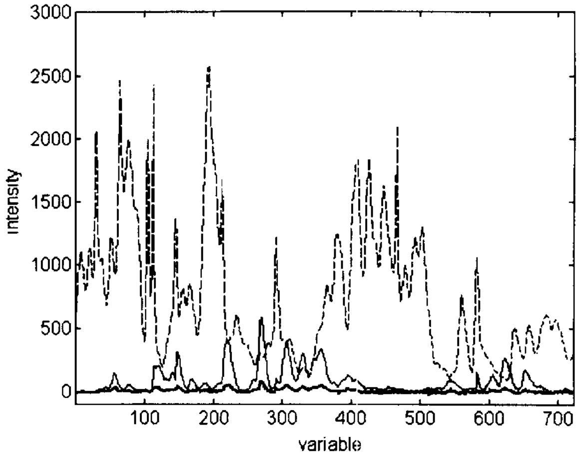

Fig. 5. Spectra of molybdenum standard solutions and the spectrum of a sample containing only the other four elements (Fe, Cr, Ni and Mn). The dashed line is the spectrum of test sample number 13, which does not contain molybdenum. The other two lines are the spectra of two molybdenum standard solutions, with concentrations of 10 mg/L and 1.5 mg/L.

of the calibration samples. In spite of the nearly complete overlapping, the absolute errors of the multivariate predictions average only 3.4%, a value that can be considered quite good, especially in view of the low Mo concentrations.

The certified samples contain small amounts of other elements, and this does not affect the quality of the predictions. A sample too different from the calibration set would be detected as an outlier by the calibration model and predictions for it would not be made.

The capability to deal with interferences, even in the high degree observed for molybdenum, is one of the advantages of the multivariate approach to calibration. Another is that the large amount of information employed in the calibration procedure usually exhibits many collinearities and redundancies in the X variables that help to stabilize predictions against noise and allow easy detection of outliers [29].

A final point is that the data acquisition step of the simultaneous multivariate methods is considerably faster. While the scanning univariate methodology takes approximately one minute to acquire the intensity values for the five elements (employing off-peak background correction on one side), the multivariate procedure described here is able to acquire the whole 81 nm spectrum in just one second.

4. Conclusions

The multivariate calibration methodology presented in this work was sucessfully applied to the simultaneous determination of manganese, molybdenum, nickel, chromium and iron in steel samples, resulting in average relative prediction errors of 2.1% for Mn, 3.4% for Mo, 0.6% for Cr, 1.5% for Ni and 0.8% for Fe. These errors are slightly smaller than those obtained with univariate calibrations and the conventional scanning detection system, and data acquisition in the new methodology is significantly faster. A central feature of the proposed procedure is the spectral window selection algorithm, which proved to be efficient and practical.

Besides the speed, typical of multidetection systems, the procedure advanced here has the versatility usually associated with scanning systems. Direct-reading spectrometers for simultaneous multielemental determination, while fast, are not adaptable. The optical arrangement is set by the manufacturer and, in spite of the effort to choose the best set of lines, it may not be adequate for all applications. In the analytical determination chosen for illustration a spectral window covering the 245–326 nm range was employed, as specified by the selection algorithm. Following the same procedure a different window could be easily selected for any other application. The width of the spectral window also could be easily modified, by exchanging the diffraction grating.

Method development, which must be done once for a given kind of sample, requires about one working day for preparing solutions, recording spectra and selecting the best spectral window. This is the price to pay for a low-cost adaptation that allows simultaneous determinations to be made on ICP sequential/single channel instruments. Further, the development time could be reduced with the use of flow systems for solution preparation and sample introduction.

Acknowledgements

The authors would like to thank FACEPE, FINEP and PADCT for partial financial support of the research reported here. PhD (MFP) and research fellowships granted by CNPq are also gratefully acknowledged.

References

[1] A. Montaser, D. W. Golightly, *Inductively Coupled Plasmas in Analytical Atomic Spectrometry*, VCH, New York, 2nd. Edn., 1992.

[2] D. Noble, *Anal. Chem.* **66**, 105A (1994).

[3] K. W. Busch, M. A. Busch, *Multielement Detection Systems for Spectrochemical Analysis*, John Wiley and Sons, New York, 1990.

[4] T. W. Barnard, M. I. Crockett, J. C. Ivaldi, P. L. Lundberg, D. A. Yates, P. A. Levine, D. J. Sauer, *Anal. Chem.* **65**, 1231 (1993).

[5] T. W. Barnard, M. I. Crockett, J. C. Ivaldi, P. L. Lundberg, *Anal. Chem.* **65**, 1225 (1993).

[6] S. Luan, H. Pang, R. S. Houk, *Spectrochim. Acta* **50B**, 791 (1995).

[7] S. W. McGeorge, E. D. Salin, *Spectrochim. Acta* **40B**, 1039 (1985).

[8] V. Karanassios, G. Horlick, *Appl. Spectrosc.* **40**, 813 (1986).

[9] G. M. Levy, A. Quaglia, R. E. Lazure, S. W. McGeorge, *Spectrochim. Acta* **42B**, 341 (1987).

[10] R. K. Winge, V. A. Fassel, M. C. Edelson, *Spectrochim. Acta* **43B**, 85 (1988).

[11] K. C. Lepla, G. Horlick, *Appl. Spectrosc.* **43**, 1187 (1989).

[12] L. Brett, R. G. Stahl, K. J. Timmins, *J. Anal. Atom. Spectrom.* **4**, 333 (1989).

[13] C. R. Belatto, J. R. Rohwedder, I. Raimundo Jr., C. Pasquini, *J. Autom.Chem.***18**, 7 (1996).

[14] E. H. van Veen, M. T. C. de Loos-Vollebregt, *Spectrochim. Acta* **45B**, 313 (1990).

[15] E. H. van Veen, F. J. Oukes, M. T. C. Loos-Vollebregt, *Spectrochim. Acta* **45B**, 1109 (1990).

[16] E. H. van Veen, M. T. C. Loos-Vollebregt, *Anal. Chem.* **63**, 1441 (1991).

[17] E. H. van Veen, M. T. C. Loos-Vollebregt, A. P, Wassink, H. Kalter, *Anal. Chem.* **64**, 1643 (1992).

[18] J. C. Ivaldi, D. Tracy, T. W. Barnard, W. Slavin, *Spectrochim. Acta* **47B**, 1361 (1992).

[19] G. Bauer, I. Rehana, W. Wegscheider, H. M. Ortner, *Spectrochim. Acta* **43B**, 971 (1988).

[20] J. Yang, Z. Piao, X. Zeng, *Spectrochim. Acta* **46B**, 953 (1991).

[21] M. Glick, K. R. Brushwyler, G. M. Hieftje, *Appl. Spectrosc.* **45**, 328 (1991).

[22] J. H. Kalivas, B. R. Kowalski, *Anal. Chem.* **53**, 2207 (1981).

[23] A. S. Al-Ammar, H. A. Hamid, B. H. Rashid, *Spectrochim. Acta* **45B**, 359 (1990).

[24] E. A. G. Zagatto, A. O. Jacintho, F. J. Krug, B. F. dos Reis, R. E. Bruns, M. C. U. Araújo, *Anal. Chim. Acta* **145**, 169 (1983).

[25] P. Zhang, D. Littlejohn, P. Neal, *Spectrochim. Acta* **48B**, 1517 (1993).

[26] P. Zhang, D. Littlejohn, *Spectrochim. Acta* **50B**, 1263 (1995).

[27] Z. Zhang, Z. Piao, X. Zeng, *Spectrochim. Acta* **48B**, 403 (1993).

[28] D. F. Wirsz, M. W. Blades, *Anal. Chem.* **58**, 51 (1986).

[29] H. Martens, T. Naes, *Multivariate Calibration*, John Wiley and Sons, London (1993).

[30] P. Geladi, B. Kowalski, *Anal. Chim. Acta* **185**, 1 (1986).

[31] W. G. Glen, W. J. Dunn III, D. R. Scott, *Tetrahedron Comp. Meth.* **2**, 349 (1989).

[32] M. Otto, W. Wegscheider, *Anal. Chem.* **57**, 63 (1985).

[33] D. C. Baxter, J. Ohman, *Spectrochim. Acta* **45B**, 481 (1990).

[34] A. Behrens, *Spectrochim. Acta* **50B**, 1521 (1995).

[35] K. Danzer, K. Venth, *Fresenius J. Anal.Chem.* **350**, 339 (1994).

[36] M. F. Pimentel, M. C. U. Araújo, B. B. Neto, C. Pasquini, *J.Autom.Chem.*, submitted.

[37] J. Cornell, *How to Run Mixture Experiments for Product Quality*, in The ASQC Basic References in Quality Control: Statistical Techniques. American Society for Quality Control, Milwaukee (1990).

[38] The Unscrambler User's Guide, version 5.0, CAMO A/S, Trondheim (1996).

[39] Matlab 4.0, The Math Works Inc., Massachussetts, USA.